



HAL
open science

Progressive Atrial Conduction Defects Associated With Bone Malformation Caused by a Connexin-45 Mutation

Akiko Seki, Taisuke Ishikawa, Xavier Daumy, Hiroyuki Mishima, Julien Barc, Ryo Sasaki, Kiyomasa Nishii, Kayoko Saito, Mari Urano, Seiko Ohno, et al.

► **To cite this version:**

Akiko Seki, Taisuke Ishikawa, Xavier Daumy, Hiroyuki Mishima, Julien Barc, et al.. Progressive Atrial Conduction Defects Associated With Bone Malformation Caused by a Connexin-45 Mutation. *Journal of the American College of Cardiology*, 2017, Equipe I, 70 (3), pp.358–370. 10.1016/j.jacc.2017.05.039 . hal-01832148

HAL Id: hal-01832148

<https://hal.science/hal-01832148>

Submitted on 12 Jul 2018

HAL is a multi-disciplinary open access archive for the deposit and dissemination of scientific research documents, whether they are published or not. The documents may come from teaching and research institutions in France or abroad, or from public or private research centers.

L'archive ouverte pluridisciplinaire **HAL**, est destinée au dépôt et à la diffusion de documents scientifiques de niveau recherche, publiés ou non, émanant des établissements d'enseignement et de recherche français ou étrangers, des laboratoires publics ou privés.

Progressive Atrial Conduction Defects Associated With Bone Malformation Caused by a Connexin-45 Mutation



Akiko Seki, MD, PhD,^{a,b} Taisuke Ishikawa, DVM, PhD,^c Xavier Daumy, PhD,^d Hiroyuki Mishima, DDS, PhD,^e Julien Barc, PhD,^d Ryo Sasaki, DDS, PhD,^f Kiyomasa Nishii, MD, PhD,^g Kayoko Saito, MD, PhD,^h Mari Urano, MA,^h Seiko Ohno, MD, PhD,ⁱ Saki Otsuki, BS,^c Hiroki Kimoto, MPharm,^c Alban-Elouen Baruteau, MD, PhD,^{d,j} Aurelie Thollet, PharmD,^k Swanny Fouchard, PhD,^k Stéphanie Bonnaud, PhD,^d Philippe Parent, MD, PhD,^l Yosaburo Shibata, MD, PhD,^m Jean-Philippe Perrin, MD,ⁿ Hervé Le Marec, MD, PhD,^{d,k} Nobuhisa Hagiwara, MD, PhD,^a Sandra Mercier, MD, PhD,^o Minoru Horie, MD, PhD,ⁱ Vincent Probst, MD, PhD,^{d,k} Koh-Ichiro Yoshiura, MD, PhD,^e Richard Redon, PhD,^{d,k} Jean-Jacques Schott, PhD,^{d,k} Naomasa Makita, MD, PhD^c

ABSTRACT

BACKGROUND Inherited cardiac conduction disease is a rare bradyarrhythmia associated with mutations in various genes that affect action potential propagation. It is often characterized by isolated conduction disturbance of the His-Purkinje system, but it is rarely described as a syndromic form.

OBJECTIVES The authors sought to identify the genetic defect in families with a novel bradyarrhythmia syndrome associated with bone malformation.

METHODS The authors genetically screened 15 European cases with genotype-negative de novo atrioventricular (AV) block and their parents by trio whole-exome sequencing, plus 31 Japanese cases with genotype-negative familial AV block or sick sinus syndrome by targeted exon sequencing of 457 susceptibility genes. Functional consequences of the mutation were evaluated using an in vitro cell expression system and in vivo knockout mice.

RESULTS The authors identified a connexin-45 (Cx45) mutation (p.R75H) in 2 unrelated families (a de novo French case and a 3-generation Japanese family) who presented with progressive AV block, which resulted in atrial standstill without ventricular conduction abnormalities. Affected individuals shared a common extracardiac phenotype: a brachyfacial pattern, finger deformity, and dental dysplasia. Mutant Cx45 expressed in Neuro-2a cells showed normal hemichannel assembly and plaque formation. However, Lucifer yellow dye transfer and gap junction conductance between cell pairs were severely impaired, which suggested that mutant Cx45 impedes gap junction communication in a dominant-negative manner. Tamoxifen-induced, cardiac-specific Cx45 knockout mice showed sinus node dysfunction and atrial arrhythmia, recapitulating the intra-atrial disturbance.

CONCLUSIONS Altogether, the authors showed that Cx45 mutant p.R75H is responsible for a novel disease entity of progressive atrial conduction system defects associated with craniofacial and dentodigital malformation. (J Am Coll Cardiol 2017;70:358-70) © 2017 by the American College of Cardiology Foundation.



Listen to this manuscript's audio summary by JACC Editor-in-Chief Dr. Valentin Fuster.



From the ^aDepartment of Cardiology, Tokyo Women's Medical University, Tokyo, Japan; ^bSupport Center for Women Health Care Professionals and Researchers, Tokyo Women's Medical University, Tokyo, Japan; ^cDepartment of Molecular Physiology, Nagasaki University Graduate School of Biomedical Sciences, Nagasaki, Japan; ^dINSERM, CNRS, UNIV Nantes, L'Institut du Thorax, Nantes, France; ^eDepartment of Human Genetics, Nagasaki University Graduate School of Biomedical Sciences, Nagasaki, Japan; ^fDepartment of Oral and Maxillofacial Surgery, Tokyo Women's Medical University, Tokyo, Japan; ^gDepartment of Anatomy and Neurobiology, National Defense Medical College, Tokorozawa, Japan; ^hInstitute of Medical Genetics, Tokyo Women's Medical University, Tokyo, Japan; ⁱDepartment of Cardiovascular and Respiratory Medicine, Shiga University of Medical Science, Otsu, Japan; ^jDepartment of Congenital Cardiology, Evelina London Children's Hospital, Guy's and St. Thomas' NHS Foundation Trust, London, United Kingdom; ^kCHU Nantes, L'Institut du thorax, Service de Cardiologie, Nantes, France; ^lCHRU Brest, Service de Génétique, Brest, France; ^mFukuoka Prefectural University, Tagawa, Japan; ⁿCHU Nantes, Service de Chirurgie Maxillo-Faciale et Stomatologie, Nantes, France; and ^oCHU Nantes, Service de Génétique Médicale, Nantes, France.

Cardiac action potentials are generated and propagated through the cardiac conduction system, which consists of the atrial conduction system (including the sinoatrial [SA] and atrioventricular [AV] nodes) and the His-Purkinje system. Proper action potential propagation is ensured by gap junctions (GJs) responsible for cell-to-cell communication. GJs consist of 3 major connexin (Cx) isoforms—Cx43, Cx40, and Cx45—each of which are characterized by chamber-specific regional distribution and permeation properties. Cx45 is strongly expressed in the early embryonic myocardium and is required for cardiac development (1). Homozygous Cx45-deficient mice are embryonic lethal; however, in the adult heart, Cx45 is expressed mainly at the SA and AV nodes and is not essential for survival of adult mice. Disease-causing mutations in GJ gamma-1 protein (*GJC1*), which encodes Cx45, have not yet been identified.

SEE PAGE 371

Dysfunction of the cardiac conduction system is primarily due to acquired conditions, such as age-related degeneration, pathological conditions, post-operative complications, and drug toxicity (2). Inherited cardiac conduction diseases (CCDs) were first described by Lenègre (3) and Lev (4) as a progressive fibrotic process in the His-Purkinje system, characterized by bundle branch blocks with wide QRS complexes, leading to complete AV block, syncope, and sudden death. CCDs are rare arrhythmia disorders that involve mutations in genes that encode cardiac ion channels (*HCN4*, *SCN5A*, *TRPM4*, *SCN1B*), membrane adaptor proteins (*ANK2*), transcription factors (*NKX2-5*, *TBX5*, *GATA4*), components of the inner nuclear membrane (*LMNA*, *EMD*), and Cx40 (*GJA5*), which all regulate action potential generation and propagation (5,6). Most CCDs are isolated cardiac conditions, but a few syndromic forms have been described, such as Andersen-Tawil syndrome (periodic paralysis) (7), Holt-Oram

syndrome (upper limb skeletal abnormalities) (8,9), and Emery-Dreifuss muscular dystrophy (muscular dystrophy) (10).

Congenital AV block is a rare arrhythmic disorder with an estimated prevalence of 1 in 14,000 to 20,000 live births (11). Transplacental passage of maternal anti-Ro-SSA and/or anti-La-SSB autoantibodies accounts for 90% to 99% of cases of congenital AV block diagnosed before 6 months of age (12). The remaining cases of congenital and childhood nonimmune AV block, without underlying structural heart disease, exhibit strong heritability (13), but the genetic basis of such idiopathic AV block is largely unknown.

To identify genetic determinants for nonimmune familial AV block, we performed trio whole-exome sequencing in 15 European cases with genotype-negative de novo AV block, as well as targeted exon sequencing of 457 CCD-susceptibility genes in 31 Japanese cases with genotype-negative familial AV block or sick sinus syndrome (SSS). We identified a Cx45 mutation, p.R75H, in 2 unrelated families: a de novo French case and a 3-generation Japanese family. Affected individuals commonly presented with progressive AV block, which resulted in atrial standstill, and was associated with an extracardiac phenotype of a brachyfacial cranial profile, finger deformity, and dental dysplasia, which suggests this is a novel disease entity of syndromic familial bradyarrhythmia.

METHODS

All individuals who were enrolled in the study gave written informed consent before genetic and clinical investigations in accordance with the standards of the Declaration of Helsinki and the local ethics committees. AV block and SSS were defined as previously described (14). Subjects with underlying structural heart diseases, acquired autoimmune diseases,

ABBREVIATIONS AND ACRONYMS

AV	= atrioventricular
CCD	= cardiac conduction disease
Cx	= connexin
ECG	= electrocardiogram/ electrocardiographic
GJ	= gap junction
N2A	= Neuro-2a
ODDD	= oculodentodigital dysplasia
PM	= pacemaker
SA	= sinoatrial
SSS	= sick sinus syndrome
WT	= wild type

Drs. Makita and Schott were supported by JSPS/CNRS Bilateral Joint Research Projects; Drs. Makita and Yoshiura were supported by the Japan Agency for Medical Research and Development (16km0405109h0004 and 15ek0109034h0002); Drs. Makita and Mishima were supported by JSPS KAKENHI (JP15H04823 and JP15K15311; JP25430183); Dr. Seki was supported by a research grant from Miwa Mikami Foundation; Dr. Ishikawa was supported by a research grant from the Takeda Science Foundation; Dr. Schott was supported by the Fondation pour la Recherche Médicale (DEQ20140329545); Dr. Redon was supported by the National Agency for Research (ANR-GENSUD-14-CE10-0001) and the Regional Council of Pays-de-la-Loire; Dr. Barc was supported by the H2020-MSCA-IF-2014 Program of the European Commission (RISTRAD-661617); and Dr. Probst was supported by the French Ministry of Health (PHRC-I PROG11/33), the Coeur et Recherche Foundation (R15074NN), and the Fédération Française de Cardiologie (RC13_0012). The authors have reported that they have no relationships relevant to the contents of this paper to disclose. Drs. Seki, Ishikawa, and Daumy contributed equally to this work. Drs. Yoshiura, Redon, Schott, and Makita jointly directed this work and are joint senior authors. Drs. Schott and Makita equally contributed as corresponding authors.

Manuscript received February 10, 2017; revised manuscript received April 29, 2017, accepted May 9, 2017.

congenital heart diseases, and other inherited arrhythmias, such as long QT syndrome and Brugada syndrome, were excluded. Electroanatomical mapping was performed, and cephalometric parameters were statistically analyzed by Ricketts' method to diagnose the facial patterns (Online Figure 1) (15).

For the trio whole-exome sequencing, we recruited a total of 15 European de novo AV block cases and their parents (Online Table 1A). Coding exons were captured from genomic DNA. For the targeted exon sequencing of conduction susceptibility genes, a total of 31 Japanese patients with familial AV block and/or SSS were recruited (Online Table 1B). Mutations in *SCN5A*, *KCNQ1*, *KCNH2*, *HCN4*, *GJA5*, *MYH6*, and *LMNA* were excluded by Sanger sequencing. Genomic DNA was captured by a custom probe panel for 457 arrhythmia susceptibility genes (Online Table 2). Raw sequence reads were aligned to the human reference genome (GRCh37). After variation calling, variations were filtered with a minor allele frequency <0.1% using public variation databases.

Lucifer yellow dye transfer experiments were conducted as previously described (16). GJ currents were recorded from Neuro-2a (N2a) cells using whole-cell double patch clamp techniques as previously described (17).

All mice were bred and used according to the procedures approved by the Animal Care and Ethics Committee at Tokyo Women's Medical University. Cx45^{fllox/fllox} mice we previously created (18) were crossed with the tamoxifen-inducible alpha-myosin heavy chain–MerCreMer transgenic mice (19) to establish time-specific conditional knockout of Cx45 gene *Gjc1* (*Gjc1*-CKO) in the heart on demand. Tamoxifen was administered intraperitoneally (1 mg/mouse) once a week 4 times, and the mice were subjected to electrophysiological study by the transesophageal pacing strategy as previously described (20). Analysis was performed on the same mice before and after tamoxifen administration. Cx45^{fllox/fllox} mice were used as the control group (Online Figure 2).

An expanded Methods section is available in the Online Appendix.

STATISTICAL ANALYSIS. Results are presented as mean ± SD unless otherwise stated, and the statistical comparisons were made using 1-way analysis of variance with Bonferroni's correction or paired Student *t* test. Statistical significance was assumed at *p* < 0.05.

RESULTS

We analyzed the clinical information for 2 families.

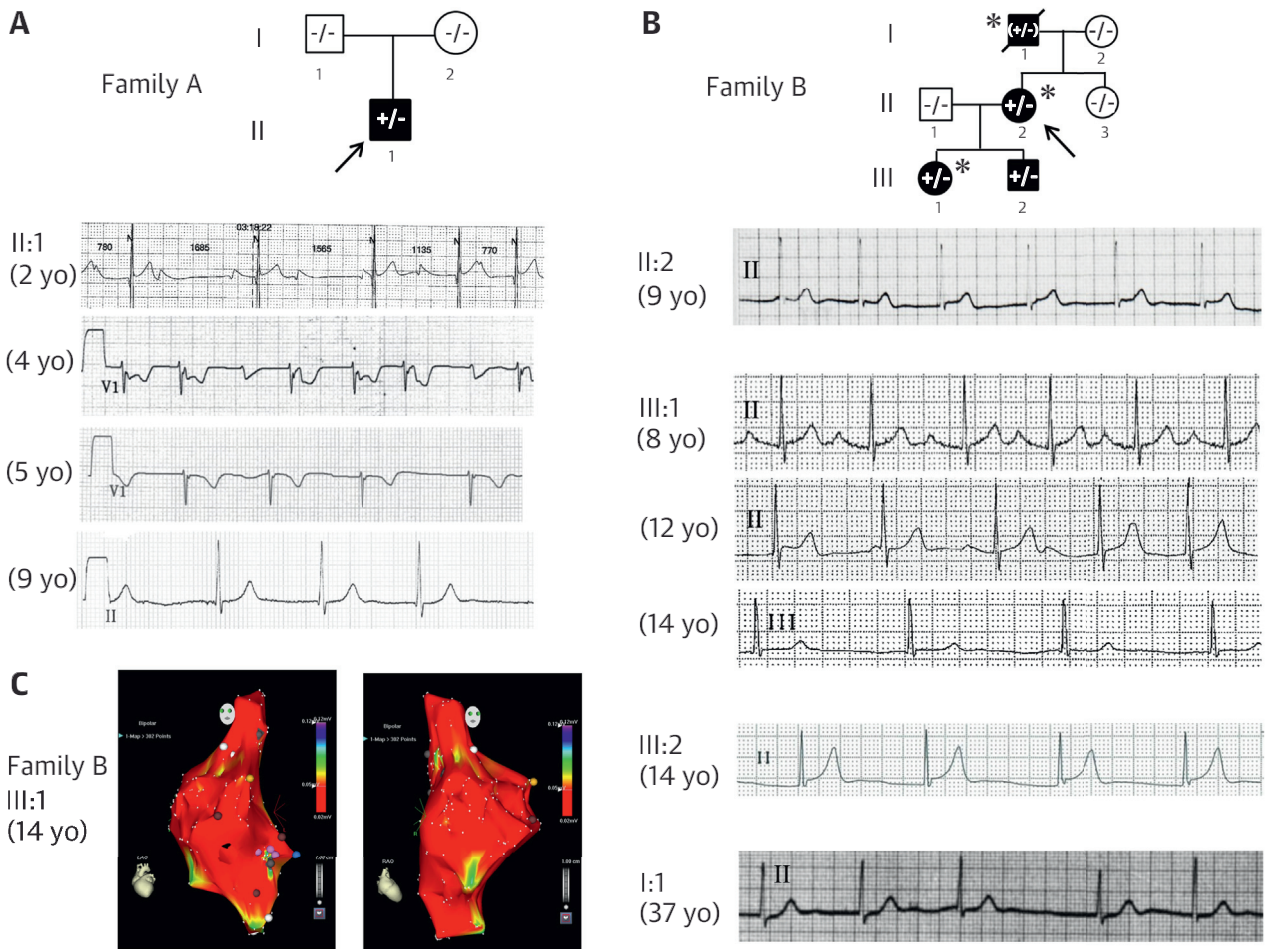
FRENCH FAMILY A. The proband of the family was a 2-year-old boy (II:1) diagnosed with first-degree AV

block at a physical examination that was initially planned for evaluating a systolic murmur. Holter electrocardiography (ECG) showed complete AV block with similar rates of P waves and QRS complexes (~100 beats/min), although he was asymptomatic (Figure 1A). He showed all degrees of AV blocks (from first to third degree), with progressively diminishing P waves that disappeared at 7 years of age. Cephalometric analysis showed a moderate brachyfacial pattern (short and wide face). He had a mild clinodactyly of the fifth finger on both hands. Dental investigation revealed mandibular permanent incisor agenesis (*n* = 5) and microdontia of bilateral maxillary lateral incisors (*n* = 2) (Figures 2A to 2C, Table 1). Both parents showed normal ECGs, and there was no family history of arrhythmia or sudden death. He is now 9 years old and asymptomatic (Online Figure 3A).

JAPANESE FAMILY B. The proband (II:2) of this family was diagnosed at 9 years of age with second-degree AV block on Holter ECG, which was performed when her father (I:1) received a permanent pacemaker (PM) implantation due to AV dissociation and atrial standstill at the age of 37 years (Figure 1B). She had several episodes of exertional dyspnea by the time she was 12 years of age, with a junctional rhythm evident by ECG. Electrophysiological study showed complete atrio-His block and partial atrial standstill; she received a PM when she was 13 years old. Additional cardiac abnormalities were not identified, but she had a remarkable family history with juvenile onset of AV block and PM implantation. Her daughter (III:1) showed first-degree AV block at 8 years of age, which progressed to AV dissociation at age 12 years (Figure 1B). P-wave amplitude diminished at 12 years of age but had disappeared by age 14 years. She had her first episode of syncope at 14 years of age. Electroanatomical mapping failed to detect voltage activities >0.05 mV in practically the entire right atrium, which is compatible with a status of atrial standstill (Figure 1C). Consequently, she underwent PM implantation. The proband's son (III:2), although asymptomatic, exhibited sinus arrest with AV junctional rhythm. Current ECGs from family members showed junctional rhythms with narrow QRS complexes (Online Figures 3B to 3D).

As extracardiac findings, the proband had a typical brachyfacial pattern. Cephalometric analysis showed markedly smaller values in midfacial length, mandibular length, and mandibular plane angle, and a substantially larger facial axis angle and facial depth angle than control subjects (Figure 2D). In addition, both hands showed camptodactyly and clinodactyly of the third to fifth fingers. X-ray further revealed brachymesophalangy (Bell type A) (Figure 2E) (21).

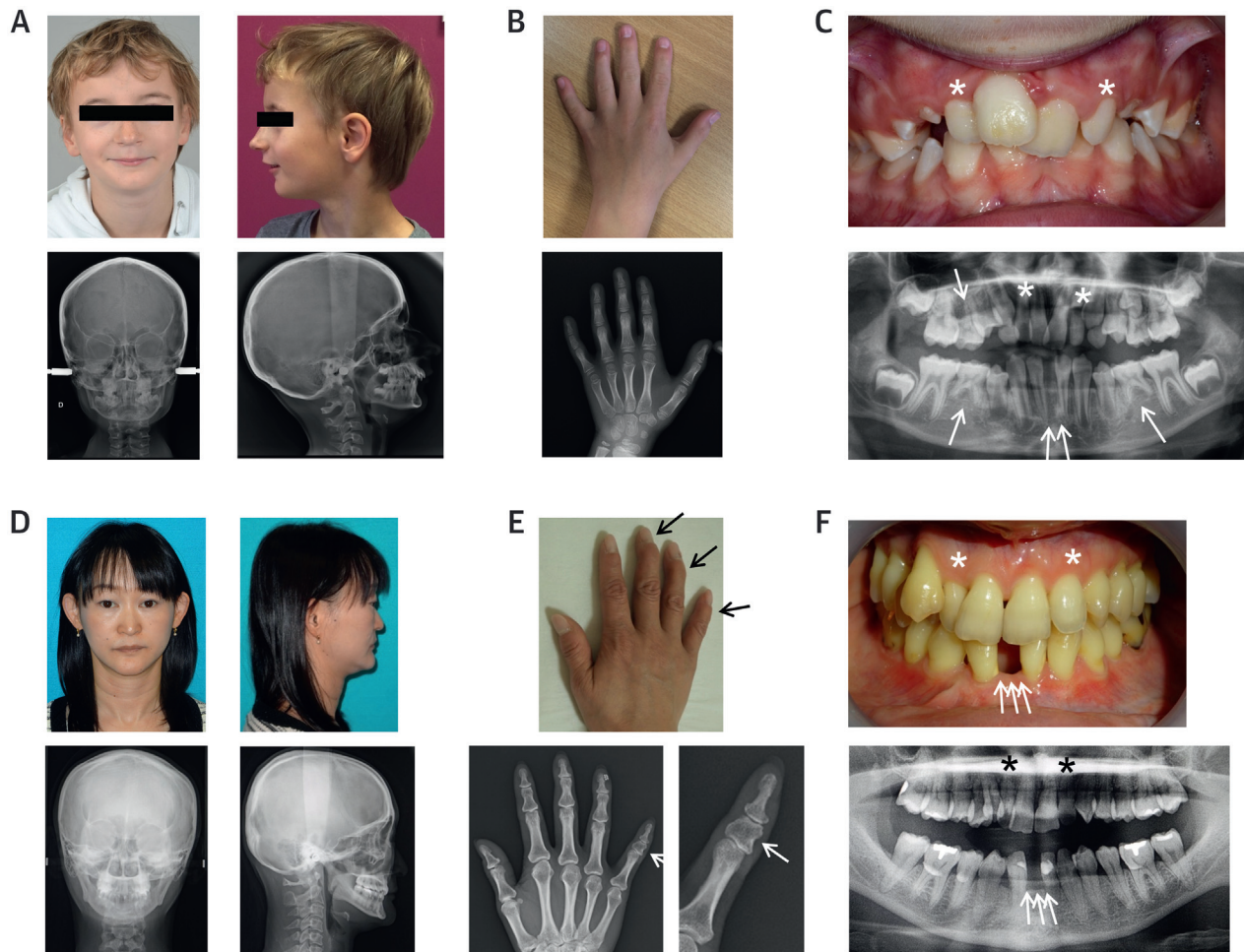
FIGURE 1 Cardiac Phenotypes of 2 Congenital AV Block Families



(A) Pedigree of a de novo case in French family A and the time course of conduction abnormalities. The proband (II:1) was initially diagnosed with first-degree atrioventricular (AV) block at 2 years of age, but Holter electrocardiogram (ECG) showed third-degree AV block with nearly identical rates of P and QRS, which had progressed to loss of P waves by the age of 9 years old (yo). **(B)** Pedigree and the conduction abnormalities of a 3-generation Japanese family B. The proband (II:2) exhibited junctional rhythm when 9 years old. Her daughter (III:1) showed first-degree AV block at 8 years of age, complete AV block at the age of 12 years, and the P waves were progressively diminished by 14 years of age. Proband's son (III:1) and deceased father (I:1) showed junctional rhythm. Asterisks and +/- represent pacemaker implantation and a status of an obligate carrier, respectively. **(C)** Three-dimensional electroanatomical mapping in III:1 of family B showed total absence of electrical activities in the right atrium (left anterior oblique [left] and right anterior oblique [right] views). Almost the entire right atrium was electrically inactive (<0.05 mV), compatible with atrial standstill.

Dental examinations showed mandibular permanent incisor agenesis and microdontia of upper lateral incisors, which were observed in 3 affected members (Figure 2F, Table 1). Permanent dental agenesis and retention of deciduous teeth were observed in the daughter and son, but was ambiguous in the proband. Microdontia was identified in the proband and daughter (Table 1, Online Figure 4). The proband's deceased father (I:1) had bilateral camptodactyly and clinodactyly (not shown); dental records were not available.

EXOME AND EXON SEQUENCING. Trios from 15 families affected by congenital AV block (n = 45) were subjected to exome sequencing, which resulted in an average depth of 84 and a mean coverage of 96.5% at 10-fold. In the proband of family A (Online Table 1A; family 12), we identified 13,035 coding variants (Table 2). Trio exome sequencing revealed 7 de novo variants, which were narrowed down to 4 rare candidate variations by filtering (minor allele frequency <0.1%) and Sanger sequencing validation (Table 3). Targeted exon sequencing of 457 conduction

FIGURE 2 Common Extracardiac Phenotypes of 2 Congenital AV Block Families

Extracardiac abnormalities are shown for (A to C) family A proband and (D to F) family B proband. (A and D) Brachyfacial pattern was demonstrated by significantly different cephalometric indexes (Table 1) for (A) family A and (D) family B probands. (B) The family A proband exhibited mild clinodactyly on the fifth fingers; (E) clinodactyly on the fifth fingers and camptodactyly on third through fifth fingers of the hand (arrows) were seen in the family B proband. (C and F) Microdontia of bilateral maxillary lateral incisor (asterisks) and mandibular permanent incisor agenesis (arrows) were observed in both probands. All photographs are reproduced with the written permission from the patients or the guardians. Abbreviations as in Figure 1.

susceptibility genes in 31 Japanese probands with congenital AV block and SSS yielded a total of 6.9-Gigs base-pairs of data, with 99.1% mapped at 239-fold coverage, and identified 1,040 coding variations in the proband of family B (Table 2; family 10 in Online Table 1B). Filtering variations by minor allele frequency <0.1% using public variation databases, Sanger validation, and family cosegregation identified 3 candidate variations (Table 3). Only *GJC1-c.G224A* (p.R75H; NM_005497), which was identified in the third exon of the *GJC1* gene encoding Cx45, was absent in public databases and

was predicted to be deleterious by in silico prediction programs (Table 3). This mutation occurred de novo in a French boy and was segregated in a 3-generation Japanese family, with all cases diagnosed with congenital AV block associated with progressive atrial standstill.

MUTANT R75H-CX45. The extracellular half of the second and fourth transmembrane helices, as well as the extracellular loops, were implicated in the intermonomer interactions of the hexameric connexons based on crystal structure analysis (22), and the

R75 was the highly conserved residue located at the junction of the first extracellular loop and the second transmembrane helix of Cx45 (Figure 3). Thus, we determined whether the R75H mutation disrupts hemichannel assembly using co-immunoprecipitation assays. Binding affinity of R75H-Cx45 was comparable to wild type (WT)-Cx45 (Figure 4A).

To investigate subcellular localization of mutant Cx45 molecules, N2a cells were transfected with myc-Cx45 plasmids containing either WT, R75H, or a combination, and labeled with green fluorescent protein-conjugated anti-myc antibody. In N2a cells that expressed WT-Cx45, the green fluorescent protein signal was mainly localized on the border between adjoining cells. The same localization was observed with cells that homozygously or heterozygously expressed R75H (Figure 4B). Capacity of GJ plaque formation (analyzed by the ratio of cell pairs with GJ plaques to the number of fluorescence-positive cell pairs) was not significantly different among the 3 groups (Online Figure 5A), which suggested that mutant Cx45 does not exhibit membrane trafficking or localization defects at the borders of adjoining cells. Combined with the co-immunoprecipitation results (Figure 4A), this indicated that similar to WT-Cx45, R75H-Cx45 can self-assemble and be transported to the cell surface to form GJ channels between adjoining cells.

To evaluate GJ permeability of mutant Cx45 channels, Lucifer yellow dye transfer was performed in N2a cell pairs that overexpressed Cx45 (either WT, R75H, or both). Immediately after rupturing the membrane to make a whole-cell patch, Lucifer yellow rapidly diffused from the pipette solution into manipulated cells (donor cells) (Figure 4C). Figure 4D shows that fluorescent intensity of the transferred dye from donor cells (open symbols) to adjoining cells (solid symbols) was time-dependent and mostly saturated within 5 minutes in almost all cells that expressed WT-Cx45. In contrast, dye transfer to adjoining cells was severely suppressed in cells that expressed homozygous (R75H) or heteromeric (WT/R75) Cx45. These findings showed that mutant Cx45 protein dominant-negatively suppressed the permeation property of WT-Cx45 protein without affecting plaque formation.

The electrophysiological properties of R75H-Cx45 were determined using dual whole-cell, patch-clamp techniques (Figure 4E). The probability of observing electrical coupling in homomeric WT-Cx45 and R75H-Cx45 was 91.7% (11 of 12) and 0% (0 of 8), respectively. Heteromeric channels (WT/R75H) expressing both WT and R75H showed electrical coupling of

TABLE 1 Extracardiac Abnormalities of French and Japanese AV Block

	Family A		Family B	
	Proband (II:1)	Proband (II:2)	Daughter (III:1)	Son (III:2)
Body measurements and cephalometric analysis*				
Sex	Male	Female	Female	Male
Current age, yrs	9	45	21	18
Body height, cm (SD/age)	129 (-0.5)	152 (-1.2)	158 (-0.1)	169 (-0.5)
Body weight, kg (SD/height)	24 (-1.3)	44 (-1.2)	52 (+0.2)	58 (-0.5)
Head circumference, cm	51.5 (-1.2)	53.5 (-0.9)	55.5 (+0.5)	56.1 (-0.3)
Midfacial length, mm	81.6 (-0.9)	71.1 (-4.7)	77.8 (-3.0)	85.5 (-2.0)
Mandibular length, mm	98.2 (-1.8)	90.3 (-6.0)	102.5 (-3.0)	116.9 (-1.2)
Facial axis angle, °	89.3 (-0.2)	93.1 (+2.0)	100.0 (+4.0)	92.6 (+1.9)
Facial depth angle, °	83.4 (-1.1)	90.6 (+0.9)	94.3 (+2.2)	96.5 (+2.5)
Mandibular plane angle, °	20.7 (-1.1)	23.5 (-1.0)	14.0 (-3.1)	17.7 (-2.0)
Facial pattern	Moderate brachyfacial	Severe brachyfacial	Severe brachyfacial	Severe brachyfacial
Dental abnormalities†				
Permanent dental agenesis	+ (5)	+ (2 or 3)	+ (2)	+ (2)
Microdontia	+ (2)	+ (2)	+ (2)	-
Retention of deciduous teeth	Ambiguous	Ambiguous	+ (2)	+ (2)

*Individual value (deviation from the mean). †Values are numbers of abnormal teeth. AV = atrioventricular; SD = standard deviation.

72.7% (8 of 11). In contrast, macroscopic conductance (G_j) measured at a transjunctional voltage (V_j) of +60 mV was significantly suppressed in heteromeric channels (WT/R75H) and homomeric channels (R75H) compared with WT (WT: 24.2 ± 7.9 nS; n = 5; WT/R75H: 4.9 ± 5.3 nS; n = 11; R75H: 0 nS; n = 8; p = 1.00 × 10⁻⁷). Steady-state G_j/V_j relationships of WT and WT/R75H were comparable (Online Figure 5B). These data showed that R75H exhibits dominant-negative suppression effects on the electrophysiological properties of WT-Cx45 channels.

TABLE 2 Filtering of Variants Identified in French and Japanese Congenital AV Block Cases

	French Case (II:1)	Japanese Case (II:2)
Target genes for exon capture	All exons (trio-exome)	457 genes
Coding variations*	13,035	1,040
De novo variants	7	NA
Minor allele frequency <0.1%	4	8
Sanger validation	4†	8
Cosegregation	NA	3
Candidate variations	4	3
Common mutation	GJCI-c.G224A, (Cx45-p.R75H)	

Values are n. *Nonsynonymous, stop-gain, stop-loss, splice site replacement, or indel frameshift. †Found in the proband (II:1) but not in his parents. AV = atrioventricular; CX45 = connexin-45; NA = not applicable.

TABLE 3 Profiles of the Rare Variations Identified in French and Japanese AV Block Families

Gene	Protein	Nucleotide	Amino Acid	Family Cosegregation	SIFT	Polyphen2	dbSNP	Minor Allele Frequency					
								1000 Genomes	ToMMo-2KJPN	ExAC	gnomAD	HGVD	
Family A (French family 12)													
<i>ZNF683</i>	Zinc finger protein 683	c.1219_1226 delCTGCACTG	p.Q407CfsX461	De novo	NA	NA	None	None	None	None	None	None	None
<i>ZNF22</i>	Zinc finger protein 22	c.C85T	p.Q29X	De novo	NA	NA	None	None	None	None	None	None	None
<i>GJC1</i>	Gap junction protein, gamma 1, 45 kDa	c.G224A	p.R75H	De novo	Damaging	PD	None	None	None	None	None	None	None
<i>ATAD2B</i>	ATPase family, AAA domain containing 2B	c.C4212G	p.L1404F	De novo	Damaging	PD	None	None	None	None	None	None	None
Family B (Japanese family 10)													
<i>CACNB2</i>	Calcium channel, voltage-dependent, beta 2 subunit	c.A305G	p.Q102R	Yes	Tolerated	PD	None	None	None	None	None	4.0E-05	None
<i>GJC1</i>	Gap junction protein, gamma 1, 45 kDa	c.G224A	p.R75H	Yes	Damaging	PD	None	None	None	None	None	None	None
<i>TTN</i>	Titin	c.G6984T	p.Q2328H	Yes	Tolerated	PD	None	None	None	None	None	4.0E-05	None

1000 Genomes (1000 Human Genome Project Database), phase 3; 2,504 individuals. ToMMo-2KJPN (Integrative Japanese Genome Variation Database from Tohoku Medical Megabank), whole-genome sequence database of 2,049 healthy Japanese individuals. ExAC (Exome Aggregation Consortium), 60,706 unrelated individuals including >33,300 non-Finnish European individuals. gnomAD (Genome Aggregation Database), 126,216 exome and 15,136 whole-genome sequences. HGVD (Human Genetic Variation Database), Japanese: 1,200 exomes.
PD = probably damaging; SIFT = Sorting Intolerant From Tolerant; other abbreviations as in Tables 1 and 2.

ECG AND ELECTROPHYSIOLOGICAL STUDY OF *GJC1*-CKO MICE. None of the basic ECG heart rate parameters (PR interval, P-wave duration, QRS interval, QTc interval, P-wave amplitude, R-wave amplitude, and T-wave amplitude) were significantly changed after tamoxifen administration in *Gjc1*-CKO (n = 9) or control mice (n = 14) (Online Table 3). After tamoxifen administration, 7 of 9 mice spontaneously showed various atrial arrhythmias, such as sinus arrhythmia, P-wave wandering, and atrial fibrillation (Figure 5A). One mouse showed prolongation of the PR interval.

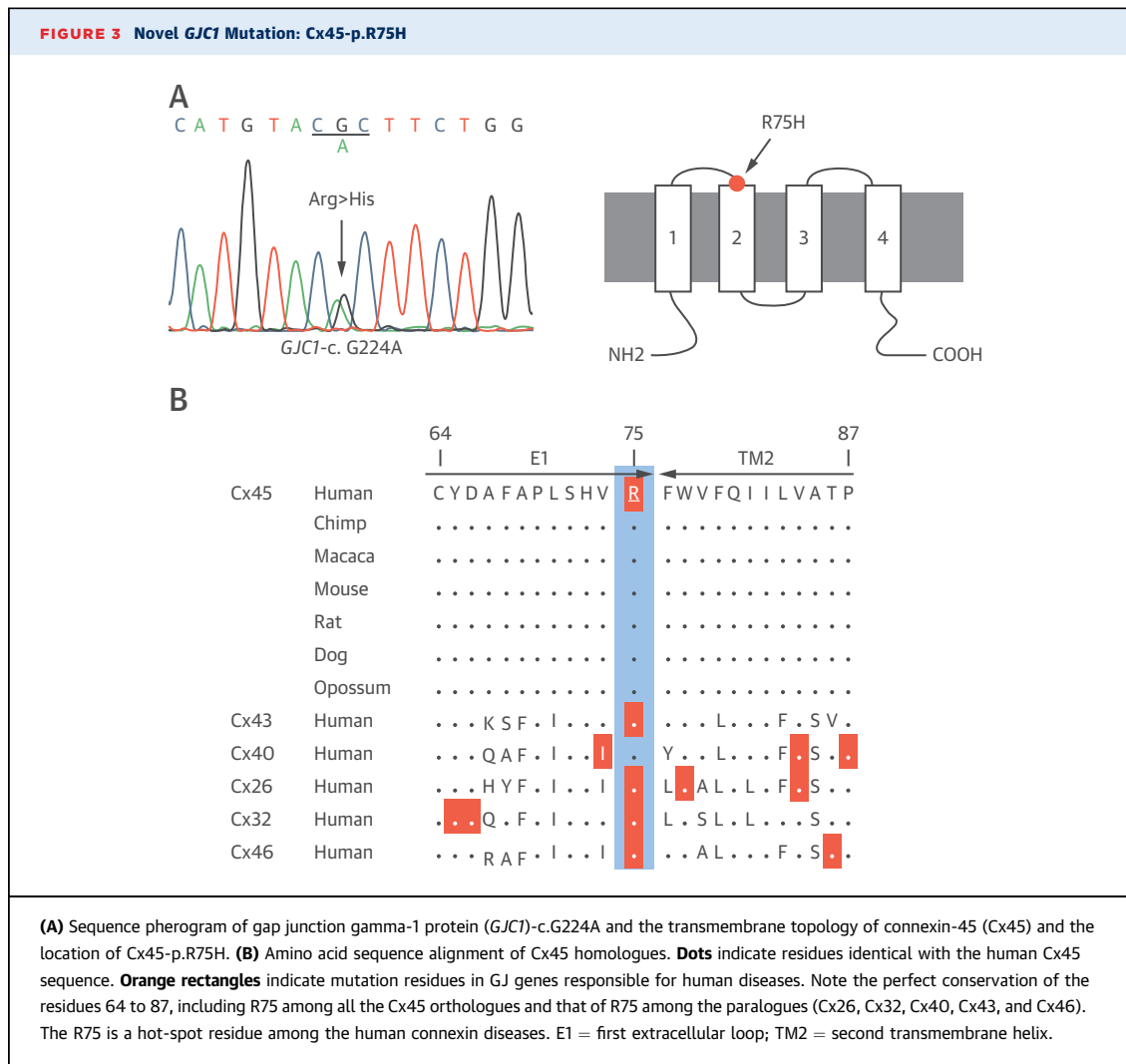
We investigated the impact of *Gjc1* depletion on SA node automaticity, AV node conductivity, and the atrial refractory period. Sinus node recovery time and corrected sinus node recovery time were significantly prolonged by tamoxifen administration despite no significant change in SA conduction time AVw (an AV node conduction parameter that represents the minimum basic cycle length causing Wenckebach type AV block), and the atrial effective refractory period was not significantly changed in *Gjc1*-CKO mice (Figures 5B to 5D, Online Table 4). Small AVw reductions after tamoxifen administration were observed in control mice, but the underlying mechanisms were not clear. There was no apparent difference in fibrosis at the SA node and AV node areas between *Gjc1*-CKO and control mice (Online Figure 6). These data implied an essential role for Cx45 in automaticity of the SA node rather than AV conduction in mice.

DISCUSSION

The CCD families presented in this study illustrated a novel familial bradyarrhythmia entity characterized by 2 clinical profiles (Central Illustration). First, conduction abnormalities in these families were limited within the atrium and nodal regions, despite the progressive nature of the fibrotic process (Online Figure 3). In contrast, most CCDs are characterized by a wide QRS complex, representing a conduction defect in the His-Purkinje or ventricular conduction systems. A CCD subtype characterized by narrow QRS was previously recognized in a large South African Caucasian family (23) and mapped to chromosome 1q32 (24). However, the genes responsible were not identified. Second, the affected members in this study exhibited nearly identical extracardiac phenotypes of craniofacial and dentodigital dysplasia, which suggested this is a syndromic form of CCD. Most CCDs are isolated cardiac conditions, but a few syndromic forms have been described, such as Andersen-Tawil syndrome (7), Holt-Oram syndrome (8,9), and Emery-Dreifuss muscular dystrophy (10).

PHENOTYPE SPECIFICITY OF CONNEXIN MUTATIONS.

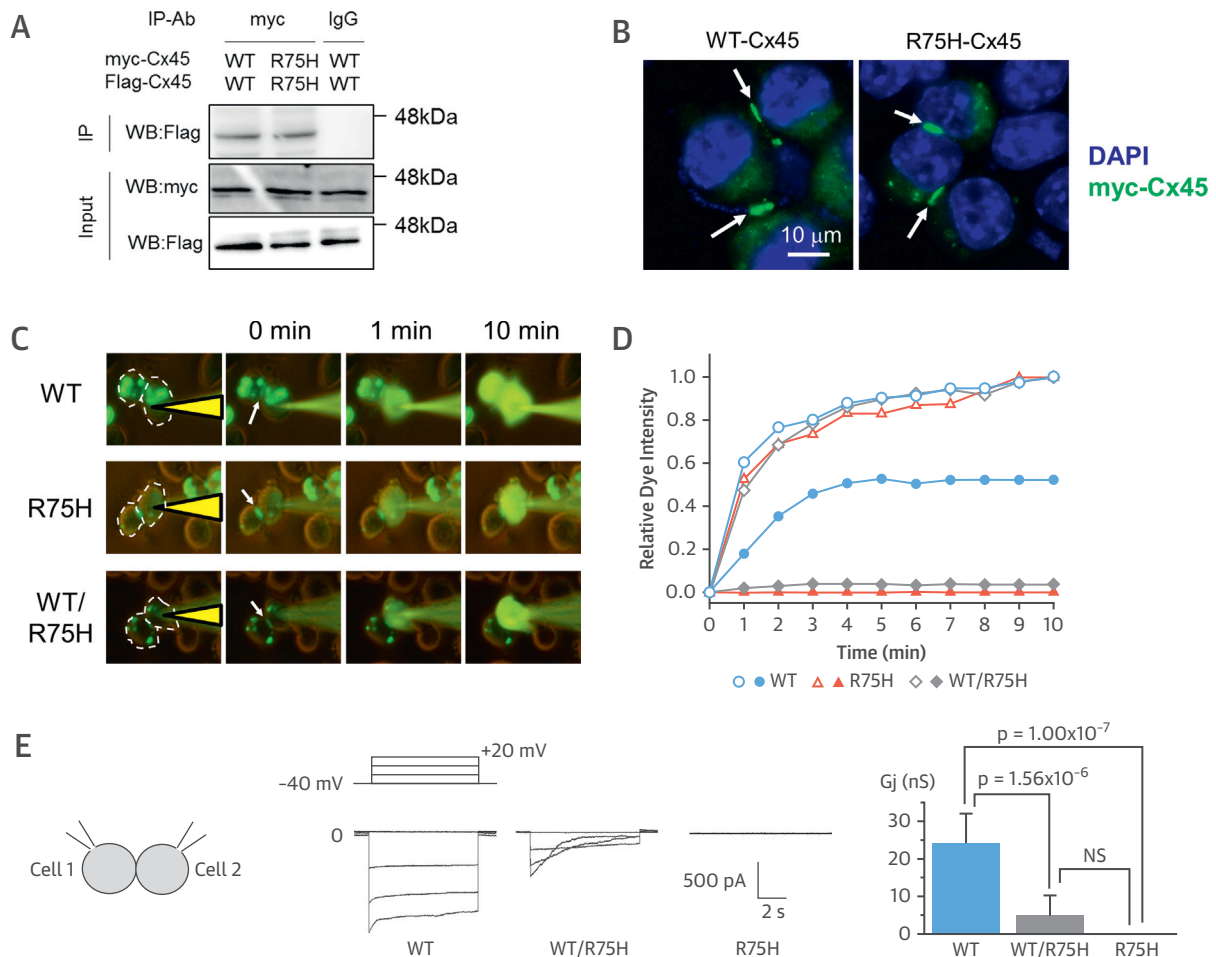
GJs electrically connect cardiomyocytes and ensure proper action potential propagation throughout the heart. Three Cx isoforms (Cx43, Cx40, and Cx45) are expressed in the human heart, each characterized by chamber-specific regional distributions and permeation properties. Cx45 constitutes the low



conductance GJ protein predominantly expressed in SA and AV nodes, whereas Cx43 is the most prevalent GJ isoform predominantly expressed in the atrium and ventricle. Mutations in Cx43 (*GJA1*) are reported in patients with oculodentodigital dysplasia (ODDD; Online Mendelian Inheritance in Man [OMIM] #164200), which is characterized by ophthalmologic, dental, and skeletal features (25). Patients with Cx43 mutations and those with Cx45-p.R75H show clinical similarity in their dental, skeletal, and craniofacial abnormalities (Table 4).

Connexins are ubiquitously expressed in almost all tissues except differentiated skeletal muscle, erythrocytes, and mature sperm cells (26). Osteoblastic cells are organized in a multicellular network, interconnected by GJs formed mainly by Cx43 and Cx45. Alterations in GJ permeability due to mutations might

modulate expression of bone matrix proteins and calcification (27,28), which, in turn, leads to the craniofacial and dentodigital abnormalities commonly observed in ODDD and Cx45 mutation carriers. In contrast to these phenotypic similarities, ophthalmological or neurological findings are observed only in ODDD, and most importantly, arrhythmias or CCD have never been reported in patients with ODDD. This might suggest that the relation between electrical coupling in an in vitro system and arrhythmogenesis in a human heart is not direct. It has been reported that Cx43 mutations not only affect the cell-to-cell coupling through a GJ-dependent mechanism, but also modulate cardiac excitability through a GJ-independent mechanism involving other molecules, such as the sodium channel and microtubules (29).

FIGURE 4 In Vitro Studies of the Novel *GJC1* Mutation

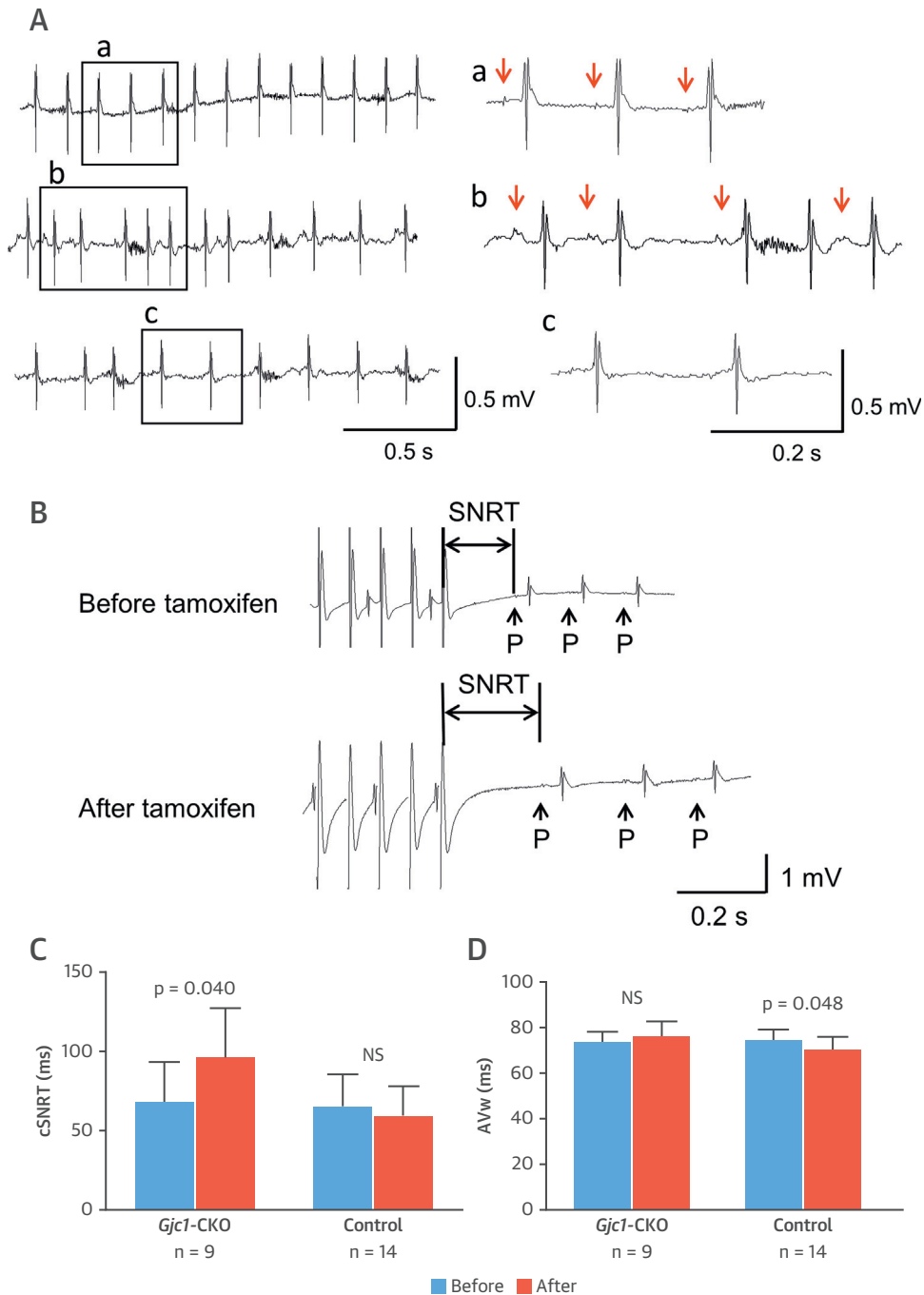
(A) Co-immunoprecipitation of myc- and flag-tagged Cx45 molecules expressed in Neuro-2a (N2a) cells was not affected by the mutation Cx45-p.R75H. **(B)** Immunofluorescent images of myc-tagged Cx45 in N2a cells showed normal expression pattern of gap junction (GJ) plaques in Cx45-p.R75H. **(C)** Time course of Lucifer yellow dye transfer in cell pairs of homomeric channels of wild type (WT) or R75H, and heteromeric WT/R75H. **(D)** Relative dye intensity of the injected cells (**open symbols**) and the adjoining cells (**solid symbols**) indicates severely impaired dye transfer in R75H and WT/R75H. **(E)** Representative current traces from the holding potential of -40 mV and stepped from -40 to $+20$ mV in 20-mV increments (**center**), and the macroscopic GJ measured at $+20$ mV (**right**). Statistical comparisons were made by 1-way analysis of variance with the Bonferroni correction. DAPI = 4',6-diamidino-2-phenylindole; IgG = control immunoglobulin G; IP-Ab = antibody for immunoprecipitation; NS = statistically not significant.

Germline mutations of GJ genes associated with CCD are extremely rare; only 1 mutation in *GJA5* (encoding Cx40) has been reported in a family with malignant CCD with His-Purkinje system disturbance, characterized by wide QRS complexes (17). The ventricular conduction defect in *GJA5* mutation carriers is in striking contrast to the progressive conduction disturbance restricted to the atrium and node in *GJC1* mutation carriers seen in this study.

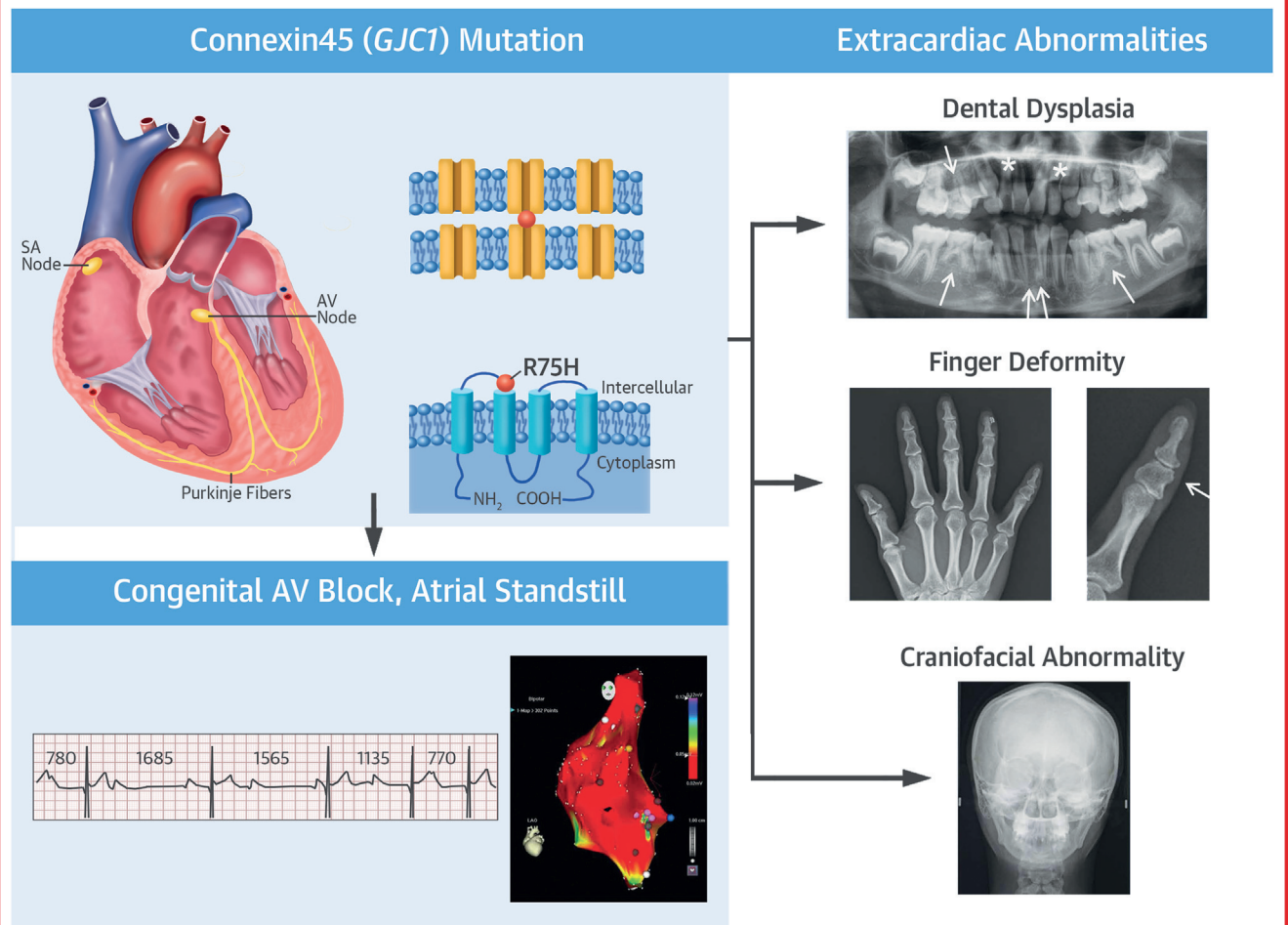
Among 5 additional rare variations identified in the 2 families (Table 3), variations of *ZNF683*, *ZNF22*, and

ATAD2B are not listed in any variation databases, and we could not exclude the possibility that these variations might modify the phenotypes of the proband of family A, which were related or unrelated to the progressive atrial conduction system defects with bone malformation. However, *GJC1*-p.R75H is the most likely disease-causing mutation because: 1) the identical mutation *GJC1*-R75H was identified in 2 unrelated families, 1 being a de novo mutation and the other showing family co-segregation; and 2) the pathological significance of this mutation was further

FIGURE 5 Electrophysiological Properties of Conditional *Gjc1* Knockout Mice



(A) Per electrocardiographic (ECG) recordings of a gap junction gamma-1 conditional knockout (*Gjc1*-CKO) mouse, atrial activities (**arrows**) frequently disappeared after tamoxifen administration; spontaneous **(a)** P-wave wandering, **(b)** sinus arrhythmia, and **(c)** junctional rhythm. **(B)** Transesophageal ECG recordings of rapid atrial pacing in an identical CKO mouse before and after tamoxifen. Sinus node recovery time (SNRT) was prolonged by tamoxifen administration. **(C)** Corrected SNRT (cSNRT) was significantly prolonged by tamoxifen administration in *Gjc1*-CKO mice, but not in control mice. **(D)** AV conduction property (AVw), the minimum basic cycle length for introducing Wenckebach AV block, was not affected by tamoxifen in *Gjc1*-CKO. Statistical comparisons were made by 1-way analysis of variance with the Bonferroni correction. Abbreviations as in [Figures 1 and 4](#).

CENTRAL ILLUSTRATION Connexin-45 Syndrome

Seki, A. et al. *J Am Coll Cardiol.* 2017;70(3):358-70.

Mutation R75H in gap junction gamma-1 protein (*GJC1*) encoding connexin-45 is responsible for a new inherited bradyarrhythmia syndrome associated with congenital atrioventricular (AV) block, progressive atrial conduction system disturbance that results in atrial standstill, and extracardiac abnormalities of craniofacial, dental, and finger dysplasia. SA = sinoatrial.

validated functionally by both in vitro and in vivo experiments. These data strongly supported that this syndrome is a Mendelian disorder with different modes of transmission.

IN VITRO AND IN VIVO EVALUATION OF CX45 MUTATION. Our in vitro experiments indicated that Cx45-p.R75H disrupted GJ permeation properties in a dominant-negative manner, despite preserving hemichannel coupling and cell-to-cell GJ plaque formation (Figure 4). The Cx45-p.R75H mutation substitutes the conserved first outer arginine residue for histidine at the junction of the first

extracellular loop and the second transmembrane helix (Figure 3). Pathophysiological relevance of the R75 residue is supported clinically by a variety of inherited diseases associated with mutations at the corresponding residue in other Cx-related diseases: ODDD (Cx43-p.R76H/S) (25,30), Charcot-Marie-Tooth disease (Cx32-p.R75Q/P/W) (31), familial hearing impairment with palmoplantar keratoderma (Cx26-p.R75Q/W) (32), and congenital cataract (Cx46-p.R76H/S) (33). Consistent with our observations, a mutagenesis study of Cx32-p.R75 demonstrated that a positive charge at this position

is required for normal channel function but not for GJ assembly (34).

Cx45 is strongly expressed in the early embryonic myocardium, and plays an essential functional role during development. Accordingly, homozygous *Gjc1*-deficient mice are embryonic lethal. In the adult heart, Cx45 is mainly restricted to SA and AV nodes. Our *Gjc1*-CKO mice exhibited intermittent spontaneous atrial pauses and SA node dysfunction after tamoxifen administration, whereas AV nodal dysfunction was not observed (Figure 5, Online Tables 3 and 4). This discrepancy of AV nodal function between patients with the *GJC1* mutation and *Gjc1*-CKO mice might reflect species differences of GJ isoform expression in the AV node. Cx30.2 (*Gjd3*) was expressed in the mouse AV node, but its orthologue Cx31.9 was not expressed in human heart (35). Further supporting this hypothesis, double-knockout mice of Cx45 and Cx30.2 showed AV node dysfunction (36).

STUDY LIMITATIONS. The underlying mechanisms of how Cx45-p.R75H causes total elimination of atrial electrical activities remain unknown. Cx45 was predominantly expressed in SA and AV nodes, as well as AV bundles of both tricuspid and mitral valves, but not in the adult heart atrium (37). It represented only 0.3% of total Cx in the adult mouse heart, but Cx45 formed heteromeric GJs with Cx43, which is abundantly expressed in the atrium and ventricles (38). Thus, it is conceivable that mutant Cx45-p.R75H suppressed function of Cx45/Cx43 heteromeric channels in a dominant-negative manner, which might disturb cell-to-cell communication of atrial cardiomyocytes, and progressively lead to total atrial standstill.

CONCLUSIONS

In summary, Cx45-p.R75H mutation caused progressive atrial conduction system dysfunction, a brachyfacial pattern, mandibular incisor agenesis, and fifth finger clinodactyly, as shown in 2 independent families. These findings revealed a previously undescribed syndrome associated with a high risk of cardiac arrhythmia.

ACKNOWLEDGMENTS The authors thank Kunio Takei for cephalometric analysis and Kenji Yoshihara for electrophysiological study of mice. The authors are grateful to Estelle Baron and Saori Nakano for their technical support. The authors would like to thank the National Referral Centre for Inherited Cardiac Arrhythmias of Nantes and its associated

TABLE 4 Comparison of Clinical Phenotypes of Families With Cx45-p.R75H and ODDD

Clinical Phenotypes	Family A	Family B			ODDD Main Features
	Proband (II:1)	Proband (II:2)	Daughter (III:1)	Son (III:2)	
Heart diseases					
Congenital AV block	+	+	+	+	-
Atrial standstill	+	+	+	+	-
Pacemaker implantation	-	+	+	-	-
Dental abnormalities					
Dental agenesis	+	+	+	+	+
Microdontia	+	+	+	-	+
Enamel hypoplasia	-	-	-	-	+
Skeletal abnormalities					
Clinodactyly	+	+	+	+	+
Brachydactyly	-	+	+	+	-
Camptodactyly	-	+	+	+	+
Syndactyly	-	-	-	-	+
Cranofacial abnormalities					
Brachyfacial pattern	+	+	+	+	+
Microcephaly	-	-	-	-	+
Narrow nose	-	-	-	-	+
Hypoplastic alae nasi	-	-	-	-	+
Prominent bridge	-	-	-	-	+
Conductive hearing loss	-	-	-	-	+/-
Ophthalmological abnormalities					
Microphthalmia	-	-	-	-	+
Microcornea	-	-	-	-	+
Neurological abnormalities					
Spastic gait/hyper-reflexia	-	-	-	-	+/-
Incontinence	-	-	-	-	+/-
Hair abnormalities					
Poor growth	-	-	-	-	+/-

ODDD = oculodentodigital dysplasia (Online Mendelian Inheritance in Man [OMIM] #164200) associated with *GJA1* mutations (25); other abbreviations as in Table 1.

competence centers. The authors acknowledge the genomics and bioinformatics core facilities of Nantes (Biogenouest) for their expert services. The authors thank the biological resource centre for biobanking (CHU Nantes, Hôtel Dieu, Centre de ressources biologiques [CRB], Nantes, F-44093, France [BRIF: BB-0033-00040]).

ADDRESSES FOR CORRESPONDENCE: Dr. Naomasa Makita, Department of Molecular Physiology, Nagasaki University Graduate School of Biomedical Sciences, 1-12-4 Sakamoto, Nagasaki 852-8523, Japan. E-mail: makitan@nagasaki-u.ac.jp. OR Dr. Jean-Jacques Schott, l'institut du thorax, Unité Inserm UMR 1087/CNRS UMR 6291, IRS-UN, 8 Quai Moncousu BP 70721 44007, Nantes Cedex 1, France. E-mail: jjschott@univ-nantes.fr.

PERSPECTIVES

COMPETENCY IN MEDICAL KNOWLEDGE: Although inherited disorders of cardiac conduction are typically isolated to the His-Purkinje system, defects in atrial conduction properties associated with Cx45 mutations might occur with or without syndromic features.

TRANSLATIONAL OUTLOOK: Further studies are needed to elucidate the mechanisms by which Cx45 mutations result in progressive atrial conduction system defects associated with craniofacial and dentodigital malformation and result in atrial standstill.

REFERENCES

- Kumai M, Nishii K, Nakamura K, Takeda N, Suzuki M, Shibata Y. Loss of connexin45 causes a cushion defect in early cardiogenesis. *Development* 2000;127:3501-12.
- Ambrosi A, Sonesson S-E, Wahren-Herlenius M. Molecular mechanisms of congenital heart block. *Exp Cell Res* 2014;325:2-9.
- Lenègre J. Etiology and pathology of bilateral bundle branch block in relation to complete heart block. *Prog Cardiovasc Dis* 1964;6:409-44.
- Lev M. The pathology of complete atrioventricular block. *Prog Cardiovasc Dis* 1964;6:317-26.
- Park DS, Fishman GI. The cardiac conduction system. *Circulation* 2011;123:904-15.
- Baruteau AE, Probst V, Abriel H. Inherited progressive cardiac conduction disorders. *Curr Opin Cardiol* 2015;30:33-9.
- Tristani-Firouzi M, Jensen JL, Donaldson MR, et al. Functional and clinical characterization of KCNJ2 mutations associated with LQT7 (Andersen syndrome). *J Clin Invest* 2002;110:381-8.
- Li QY, Newbury-Ecob RA, Terrett JA, et al. Holt-Oram syndrome is caused by mutations in TBX5, a member of the Brachyury (T) gene family. *Nat Genet* 1997;15:21-9.
- Basson CT, Bachinsky DR, Lin RC, et al. Mutations in human TBX5 cause limb and cardiac malformation in Holt-Oram syndrome. *Nat Genet* 1997;15:30-5.
- Nagano A, Koga R, Ogawa M, et al. Emerin deficiency at the nuclear membrane in patients with Emery-Dreifuss muscular dystrophy. *Nat Genet* 1996;12:254-9.
- Michaelsson M, Engle MA. Congenital complete heart block: an international study of the natural history. *Cardiovasc Clin* 1972;4:85-101.
- Chameides L, Truex RC, Vetter V, Rashkind WJ, Galio FM Jr., Noonan JA. Association of maternal systemic lupus erythematosus with congenital complete heart block. *N Engl J Med* 1977;297:1204-7.
- Baruteau AE, Behaghel A, Fouchard S, et al. Parental electrocardiographic screening identifies a high degree of inheritance for congenital and childhood nonimmune isolated atrioventricular block. *Circulation* 2012;126:1469-77.
- Olgin JE, Zipes DP. Specific arrhythmias: diagnosis and treatment. In: Braunwald E, Zipes DP, Libby P, editors. *Heart Disease: A Textbook of Cardiovascular Medicine*. Philadelphia: Saunders, 2001:815-99.
- Ricketts RM, Bench RW, Gugino CF, Hilgers JJ, Schulhof RJ. Bioprogressive therapy. Denver, CO: Rocky Mountain Orthodontics, 1979:59.
- Piazza V, Beltramello M, Menniti M, et al. Functional analysis of R75Q mutation in the gene coding for connexin 26 identified in a family with non-syndromic hearing loss. *Clin Genet* 2005;68:161-6.
- Makita N, Seki A, Sumitomo N, et al. A connexin40 mutation associated with a malignant variant of progressive familial heart block type I. *Circ Arrhythm Electrophysiol* 2012;5:163-72.
- Nishii K, Seki A, Kumai M, et al. Connexin45 contributes to global cardiovascular development by establishing myocardial impulse propagation. *Mech Dev* 2016;140:41-52.
- Sohal DS, Nghiem M, Crackower MA, et al. Temporally regulated and tissue-specific gene manipulations in the adult and embryonic heart using a tamoxifen-inducible Cre protein. *Circ Res* 2001;89:20-5.
- Hagendorff A, Schumacher B, Kirchhoff S, Luderitz B, Willecke K. Conduction disturbances and increased atrial vulnerability in Connexin40-deficient mice analyzed by transesophageal stimulation. *Circulation* 1999;99:1508-15.
- Bell J. *Brachydactyly and Symphalangism*. London: Cambridge University Press, 1951.
- Maeda S, Nakagawa S, Suga M, et al. Structure of the connexin 26 gap junction channel at 3.5 Å resolution. *Nature* 2009;458:597-602.
- Brink AJ, Torrington M. Progressive familial heart block—two types. *S Afr Med J* 1977;52:53-9.
- Fernandez P, Moolman-Smook J, Brink P, Corfield V. A gene locus for progressive familial heart block type II (PFHBII) maps to chromosome 1q32.2-q32.3. *Hum Genet* 2005;118:133-7.
- Paznekas WA, Boyadjiev SA, Shapiro RE, et al. Connexin 43 (GJA1) mutations cause the pleiotropic phenotype of oculodentodigital dysplasia. *Am J Hum Genet* 2003;72:408-18.
- Nielsen MS, Axelsen LN, Sorgen PL, Verma V, Delmar M, Holstein-Rathlou NH. Gap junctions. *Compr Physiol* 2012;2:1981-2035.
- Lecanda F, Towler DA, Ziambaras K, et al. Gap junctional communication modulates gene expression in osteoblastic cells. *Mol Biol Cell* 1998;9:2249-58.
- Laing JG, Manley-Markowski RN, Koval M, Civitelli R, Steinberg TH. Connexin45 interacts with zonula occludens-1 and connexin43 in osteoblastic cells. *J Biol Chem* 2001;276:23051-5.
- Agullo-Pascual E, Lin X, Leo-Macias A, et al. Super-resolution imaging reveals that loss of the C-terminus of connexin43 limits microtubule plus-end capture and NaV1.5 localization at the intercalated disc. *Cardiovasc Res* 2014;104:371-81.
- Pizzuti A, Flex E, Mingarelli R, Salpietro C, Zelante L, Dallapiccola B. A homozygous GJA1 gene mutation causes a Hallermann-Streiff/ODDD spectrum phenotype. *Hum Mutat* 2004;23:286.
- Yum SW, Kleopa KA, Shumas S, Scherer SS. Diverse trafficking abnormalities of connexin32 mutants causing CMTX. *Neurobiol Dis* 2002;11:43-52.
- Yum SW, Zhang J, Scherer SS. Dominant connexin26 mutants associated with human hearing loss have trans-dominant effects on connexin30. *Neurobiol Dis* 2010;38:226-36.
- Burdon KP, Wirth MG, Mackey DA, et al. A novel mutation in the connexin46 gene causes autosomal dominant congenital cataract with incomplete penetrance. *J Med Genet* 2004;41:e106.
- Abrams CK, Islam M, Mahmoud R, Kwon T, Bargiello TA, Freidin MM. Functional requirement for a highly conserved charged residue at position 75 in the gap junction protein connexin 32. *J Biol Chem* 2013;288:3609-19.
- Kreuzberg MM, Liebermann M, Segschneider S, et al. Human connexin31.9, unlike its orthologous protein connexin30.2 in the mouse, is not detectable in the human cardiac conduction system. *J Mol Cell Cardiol* 2009;46:553-9.
- Frank M, Wirth A, Andrie RP, et al. Connexin45 provides optimal atrioventricular nodal conduction in the adult mouse heart. *Circ Res* 2012;111:1528-38.
- Yamamoto M, Dobrzynski H, Tellez J, et al. Extended atrial conduction system characterised by the expression of the HCN4 channel and connexin45. *Cardiovasc Res* 2006;72:271-81.
- Bao M, Kanter EM, Huang RY, et al. Residual Cx45 and its relationship to Cx43 in murine ventricular myocardium. *Channels (Austin)* 2011;5:489-99.

KEY WORDS brachyfacial pattern, congenital atrioventricular block, connexin-45, dentodigital dysplasia, knockout mice, whole-exome sequencing

APPENDIX For expanded Methods and Results sections as well as supplemental tables and figures, please see the online version of this article.